Journal of Alzheimer's Disease 7 (2005) 63–80
IOS Press

Impaired insulin and insulin-like growth factor expression and signaling mechanisms in Alzheimer's disease – is this type 3 diabetes?

Eric Steen, Benjamin M. Terry, Enrique J. Rivera, Jennifer L. Cannon, Thomas R. Neely, Rose Tavares, X. Julia Xu, Jack R. Wands and Suzanne M. de la Monte *
From the Departments of Pathology and Medicine, Rhode Island Hospital and Brown Medical School, Providence, RI, USA

Abstract. The neurodegeneration that occurs in sporadic Alzheimer's disease (AD) is consistently associated with a number of characteristic histopathological, molecular, and biochemical abnormalities, including cell loss, abundant neurofibrillary tangles and dystrophic neurites, amyloid-β deposits, increased activation of pro-death genes and signaling pathways, impaired energy metabolism/mitochondrial function, and evidence of chronic oxidative stress. The general inability to convincingly link these phenomena has resulted in the emergence and propagation of various heavily debated theories that focus on the role of one particular element in the pathogenesis of all other abnormalities. However, the accumulating evidence that reduced glucose utilization and deficient energy metabolism occur early in the course of disease, suggests a role for impaired insulin signaling in the pathogenesis of AD. The present work demonstrates extensive abnormalities in insulin and insulin-like growth factorm typer I and II (IGF-I and IGF-II) signaling mechanisms in brains with AD, and shows that while each of the corresponding growth factors is normally made in central nervous system (CNS) neurons, the expression levels are markedly reduced in AD. These abnormalities were associated with reduced levels of insulin receptor substrate (IRS) mRNA, *tau* mRNA, IRS-associated phosphotidylinositol 3-kinase, and phospho-Akt (activated), and increased glycogen synthase kinase-3β activity and amyloid precursor protein mRNA expression. The strikingly reduced CNS expression of genes encoding insulin, IGF-I, and IGF-II, as well as the insulin and IGF-I receptors, suggests that AD may represent a neuro-endocrine disorder that resembles, yet is distinct from diabetes mellitus. Therefore, we propose the term, "Type 3 Diabetes" to reflect this newly identified pathogenic mechanism of neurodegeneration.

Keywords: Diabetes, insulin signaling, insulin gene expression, central nervous system, Alzheimer's disease, glycogen synthase kinase, growth factor receptors, real time RT-PCR

1. Introduction

The characteristic neuropathological and molecular lesions that correlate with dementia in Alzheimer's Disease (AD) include the accumulation of hyperphosphorylated and poly-ubiquitinated microtubule-associated proteins, such as *tau*, resulting in the formation of neurofibrillary tangles, dystrophic neuritis, and neuropil threads. Neuronal cytoskeletal abnormalities are associated with cerebral atrophy with cell and fiber loss, and synaptic disconnection. Increased amyloid-beta (Aβ) deposition around and within the walls of meningeal and cortical vessels, the cortical neuropil, and neuronal perikarya is a feature of both AD and

*Corresponding author: Dr. Suzanne M. de la Monte, Pierre Galletti Research Building, Rhode Island Hospital, 55 Claverick Street, Room 419, Providence, RI 02903, USA. Tel.: +1 401 444 7364; Fax: +1 401 444 2939; E-mail: Suzanne_DeLaMonte_MD@Brown.edu.

ISSN 1387-2877/05/$17.00

normal aging. Although genetic factors can predispose individuals to develop premature and excessive cerebral deposits of Aβ, most cases of AD-type dementia are sporadic and do not exhibit clear familial or genetic clustering. Recent exploration of biochemical, molecular, and cellular abnormalities that precede or accompany classic AD demonstrated that cell loss was associated with increased activation of pro-death genes and signaling pathways, impaired energy metabolism, mitochondrial dysfunction, chronic oxidative stress, and cerebrovascular disease/cerebral hypoperfusion. However, the inability to interlink these phenomena under a single primary pathogenic mechanism resulted in the emergence and propagation of various heavily debated theories, each of which is focused on how one particular component of AD could trigger a cascade that contributes to the development of all other known abnormalities. However, re-evaluation of some of the older literature revealed that impairments in cerebral glucose utilization and energy metabolism represent very early abnormalities that precede or accompany the initial stages of cognitive impairment. This concept truly warrants revisiting, particularly in light of the emerging evidence that impaired insulin signaling may have an important role in the pathogenesis of AD.

Currently, there is a growing interest in clarifying the roles of insulin resistance, hyperinsulinemia, Type 2 Diabetes Mellitus, and insulin degrading enzyme in the pathogenesis of AD, and its associated neuronal cytoskeletal lesions and Aβ deposits in the brain [1–11]. This relatively new wave of enthusiasm is being fueled by reports showing reduced brain growth and increased *tau* phosphorylation in mice deficient in either the insulin receptor substrate-2 [10,11] or the neuronal insulin receptor [11] gene. The potential role of the neuroendocrine system in AD was raised 15 to 20 years ago when abnormalities in the hypothalamic-pituitary axis were detected [12–17]. That concept nearly vanished with the tidal wave of accelerated research on Aβ and *tau*, although presently, the renewed interest in neuroendocrine mechanisms emphasizes systemic disease rather than intrinsic CNS endocrine dysfunction. However, previous research in our laboratory revealed that many important components of CNS neurodegeneration that occur in AD are mediated by impaired insulin signaling in the brain [18–21]. The present study was designed to characterize and quantify AD-associated abnormalities in insulin and insulin-like growth factor (IGF) peptide and receptor gene expression, and the corresponding downstream signaling mechanisms that mediate neuronal survival using human AD and aged control postmortem brain tissue.

Herein, we demonstrate that insulin, IGF-I, and IGF-II peptides and receptors are all expressed in the brain, and that AD is associated with striking reductions in both insulin and IGF-I mRNA expression, and down-regulation of the corresponding receptors. The signaling pathways that mediate insulin and IGF-I stimulated survival signaling were also probed. The study design utilized highly sensitive real time quantitative reverse transcribed polymerase chain reaction (RT-PCR) amplification assays, which were highly efficient for detecting alterations in gene expression in postmortem brain tissue. The aggregate results suggest that the insulin/IGF-I signaling abnormalities in AD do not correspond to either Type 1 or Type 2 diabetes, but rather reflect a different and more complex disease process that originates in the CNS.

2. Methods

2.1. Source of tissue

Postmortem brain tissue was obtained from the Massachusetts General Hospital Alzheimer Disease Research Center (ADRC) brain bank, the Brown University Brain Bank, and the Kathleen Price Bryan Brain Bank at Duke University Medical Center. The diagnoses of AD (Braak and Braak Stages V-VI) and normal aging (Braak and Braak Stages 0-I) [22,23] were confirmed by review of the clinical histories and postmortem histopathological sections of brain, including the Bielschowsky stained, and phospho-Tau, ubiquitin, and amyloid-β immunostained sections of pre-frontal cortex, temporal cortex, amygdala, and hippocampus. Snap frozen tissues ($\sim$100 mg each) from the hippocampus, hypothalamus, frontal lobe (Brodmann Area 11), and cerebellar cortex were used to extract RNA and protein. Adjacent formalin fixed paraffin-embedded tissue blocks were used for immunohistochemical staining. A total of 28 AD and 26 control cases were included in this study. Postmortem intervals were all less than 14 hours. Cases were rejected if RNA degradation was detected by real time quantitative RT-PCR.

2.2. Real time quantitative RT-PCR

Total RNA was isolated from brain tissue using TRIzol reagent (Invitrogen, Carlsbad, CA) according to the manufacturer's protocol. RNA concentrations were determined from the absorbances measured at 260 nm

and 280 nm. RNA (2 μg) was reverse transcribed using the AMV First Strand cDNA synthesis kit (Roche Diagnostics Corporation, Indianapolis, IN) and random oligodeoxynucleotide primers. The mRNA levels of insulin, IGF-I, and IGF-II growth factors, their corresponding receptors, insulin receptor substrate (IRS) subtypes 1, 2, and 4, *tau*, amyloid precursor protein (APP), glucose transporter 4 (GLUT4), and insulin degrading enzyme (IDE) were measured using real time quantitative RT-PCR amplification. Ribosomal 18S RNA levels measured in parallel reactions were used to calculate relative abundance of each mRNA transcript [21,24]. Ribosomal 28S RNA levels were also measured and the corresponding 28S/18S ratios were calculated to further assess RNA integrity.

PCR amplifications were performed in 25 μl reactions containing cDNA generated from 2.5 ng of original RNA template, 300 nM each of gene specific forward and reverse primer (Table 1), and 12.5 μl of 2x QuantiTect SYBR Green PCR Mix (Qiagen Inc, Valencia, CA). The amplified signals were detected continuously with the BIO-RAD iCycler iQ Multi-Color RealTime PCR Detection System (Bio-Rad, Hercules, CA). The amplification protocol used was as follows: initial 15-minutes denaturation and enzyme activation at 95°C, 40 cycles of 95°C $\times$ 30 sec, 55°–60°C $\times$ 45 sec, and 72°C $\times$ 60 sec. Annealing temperatures were optimized using the temperature gradient program provided with the iCycler software. The mRNA levels were determined using the equations of the regression lines generated with serial 10-fold dilutions of 20 ng of recombinant plasmid DNA containing the target sequences studied. Relative mRNA abundance was determined from the ng ratios of specific mRNA to18S [21, 24].

In preliminary studies, SYBR Green-labeled PCR products were evaluated by agarose gel electrophoresis, and the authenticity of each amplicon was verified by nucleic acid sequencing. Serial dilutions of known quantities of recombinant plasmid DNA containing the specific target sequences were used as standards in the PCR reactions, and the regression lines generated from the Ct values of the standards were used to calculate mRNA abundance. Results were normalized with respect to 18S RNA because the levels were highly abundant and essentially invariant, whereas housekeeping genes were modulated with disease state. Between-group statistical comparisons were made using the calculated mRNA/18S ratios.

2.2.1. Western blot analysis

Western blot analysis was used to assess the levels of Akt, phospho-Akt, GSK-3β, phospho-GSK-3β, Tau, and α-actin. Fresh frozen tissue ($\sim$100 mg) was homogenized in 5 volumes of radio-immunoprecipitation assay (RIPA) buffer (50 mM Tris-HCl, pH 7.5, 1% NP-40, 0.25% Na-deoxycholate, 150 mM NaCl, 1 mM EDTA, 2 mM EGTA) containing protease (1 mM PMSF, 0.1 mM TPCK, 1 μg/ml aprotinin, 1 μg/ml pepstatin A, 0.5 μg/ml leupeptin, 1 mM NaF, 1 mM $Na_4P_2O_7$) and phosphatase (2 mM Na_3VO_4) inhibitors. Protein concentration was determined using the bicinchoninic acid (BCA) assay (Pierce, Rockford, IL). Samples containing 100 μg of protein were fractionated by sodium dodecyl sulfate, polyacrylamide gel electrophoresis (SDS-PAGE) [25]. Proteins were transferred to Immobilon-P (Millipore Corporation, Bedford, MA) PVDF membranes and non-specific binding sites were adsorbed with SuperBlock-TBS (Pierce, Rockford, IL). Membranes were incubated over night at 4°C with primary antibody (0.5–1 μg/ml) diluted in Tris-buffered saline (TBS; 50 mM Tris, 150 mM NaCl, pH 7.4) containing 1% bovine serum albumin and 0.05% Tween-20 (TBST-BSA). Immunoreactivity was detected using horseradish peroxidase (HRP) conjugated IgG (Pierce, Rockford, IL), Western Lightning chemiluminescence reagents (Perkin Elmer Life Sciences Inc., Boston, MA), and film autoradiography. All incubations were performed using gentle platform agitation. Immunoreactivity was quantified using the Kodak Digital Science Imaging Station (NEN Life Sciences, Boston, MA).

2.3. Immunoprecipitation

Immunoprecipitation studies were used to examine interactions between the p85 subunit of PI3 kinase and insulin receptor substrate (IRS) types 1 and 2. The tissue samples were homogenized in RIPA buffer containing protease and phosphatase inhibitors (1 μg/ml aprotinin, 0.5 μg/ml leupeptin, 1 mM PMSF, 0.1 mM TPCK, 1 μg/ml pepstatin A, 2 mM sodium vanadate), and diluted in HEPES lysis buffer containing 10 mM HEPES, 100 mM NaCl, 1 mM EDTA, and 0.1% Triton X-100 just prior to use in immunoprecipitation assays. After pre-clearing, samples containing 250 μg of protein were incubated with primary antibody for 2 hours at 4°C with constant rotation. Immune complexes were captured on UltraLink immobilized Protein A/G (Pierce, Rockford, IL) by a two-hour incubation at 4°C with gentle rotation. The immunopre-

cipitates were washed 3 times in 0.5 ml of Hepes lysis buffer [25], and then used in kinase assays or Western blot analyses.

2.4. Immunocytochemical staining

Buffered formalin-fixed, paraffin-embedded sections (8 μM thick) of hypothalamus and temporal or frontal neocortex were immunostained with antibodies to insulin receptor, IGF-I receptor, insulin, and IGF-I using the avidin biotin horseradish peroxidase method and either NovaRed or diaminobenzidine (Vector Laboratories, Burlingame, CA) as the chromogen [26]. The sections were counterstained with hematoxylin and examined by light microscopy.

2.5. Source of reagents

Antibodies to insulin receptor, IGF-I receptor, IRS-1, IRS-2, and the p85 subunit of PI3 kinase were obtained from Cell Signaling (Beverly, MA). Antibodies to GSK-3β, Akt, and phospho-specific antibodies to GSK-3α/β (Ser21/9) and Akt (Ser473 and Thr308) were purchased from Cell Signaling Technology, Beverly, MA). Protein A/G agarose was obtained from Pierce Chemical Company (Rockford, IL). Reagents for immunohistochemical staining were purchased from Vector Laboratories, (Burlingame, CA). All other fine chemicals were purchased from either CalBiochem (Carlsbad, CA) or Sigma-Aldrich (St. Louis, MO).

2.6. Statistical analysis

Data depicted in the graphs represent the means $\pm$ S.E.M.'s for each group. Inter-group comparisons were made using Student t-tests or repeated measures analysis of variance (ANOVA) with the Tukey-Kramer post-hoc test for significance. Statistical analyses were performed using the Number Cruncher Statistical System (Dr. Jerry L. Hintze, Kaysville, UT). The computer software generated P-values are indicated in the graphs. P-values < 0.05 were regarded as statistically significant.

3. Results

3.1. General comments regarding postmortem specimens

The use of real time quantitative RT-PCR enabled all samples to be analyzed simultaneously and with sufficient replicates to demonstrate consistency of results. With the techniques employed, the quality of the cDNA templates generated from human postmortem brain was judged to be excellent based on the similar 18S Ct values and consistent 28S:18S ratios obtained for both the control and AD cases, and the comparability of these values to those obtained for RNA isolated from experimental animal tissues or primary neuronal cultures. Typically, with cDNA prepared from 10 ng of total RNA, the 18S Ct values ranged from 8–10, and the calculated 28S/18S ng ratios ranged from 2.0 to 2.2 as previously reported for postmortem brain tissue using Northern blot or slot blot analysis [27,28]. This approach is also ideally suited for rigorous quantitative analysis of gene expression in postmortem brain tissue because the amplicons are small ($<$ 150 bp), thereby circumventing any potential problems related to partial RNA degradation, e.g. nicking, which may increase with postmortem delay or sample processing. Moreover, the specificity of the amplified products can be verified by direct nucleic acid sequencing.

3.2. Reduced growth factor receptor expression in AD

Real time quantitative RT-PCR studies demonstrated mRNA transcripts corresponding to insulin, IGF-I, and IGF-II receptors in the cerebral cortex, hippocampus, hypothalamus, and cerebellar cortex of both control and AD brains (Fig. 1). Insulin, IGF-I and IGF-II receptors were expressed at 400- to 2000-fold higher levels in the hippocampus and hypothalamus than in the frontal cortex. IGF-I and IGF-II receptors were overall more abundantly expressed than insulin receptors. In control frontal cortex and hypothalamus, IGF-I receptors were more abundantly expressed than IGF-II receptors, whereas in the hippocampus, the expression levels of these receptors were similar. As observed in the control group, the IGF-I receptor was more abundantly expressed than the IGF-II receptor in AD frontal cortex. However, IGF-II receptor expression was increased relative to IGF-I receptor in AD hippocampus (Fig. 1B). In both control and AD cerebella, IGF-I receptors were more abundantly expressed than IGF-II receptors (Table 2).

Table 1
Primer pairs for real time quantitative RT-PCR analysis of human brain tissue*

Primer	Sequence (5′–>3′)	Position (mRNA)	Amplicon size (bp)
Insulin	TTC TAC ACA CCC AAG TCC CGT C	189	134
	ATC CAC AAT GCC ACG CTT CTG C	322	
Insulin receptor	GGT AGA AAC CAT TAC TGG CTT CCT C	1037	125
	CGT AGA GAG TGT AGT TCC CAT CCA C	1161	
IGF-I	CAC TTC TTT CTA CAC AAC TCG GGC	1032	147
	CGA CTT GCT GCT GCT TTT GAG	1178	
IGF-I receptor	AGG GCG TAG TTG TAG AAG AGT TTC C	395	101
	TAC TTG CTG CTG TTC CGA GTG G	295	
IGF-II	CTG ATT GCT CTA CCC ACC CAA G	996	76
	TTG CTC ACT TCC GAT TGC TGG C	1071	
IGF-II receptor	CAC GAC TTG AAG ACA CGC ACT TAT C	403	132
	GCT GCT CTG GAC TCT GTG ATT TG	534	
IRS-1	TGC TGG GGG TTT GGA GAA TG	3559	68
	GGC ACT GTT TGA AGT CCT TGA CC	3626	
IRS-2	AAA ATT GGC GGA GCA AGG C	753	64
	ATG TTC AGG CAG CAG TCG AGA G	816	
IRS-4	CCG ACA CCT CAT TGC TCT TTT C	570	74
	TTT CCT GCT CCG ACT CGT TCT C	643	
Tau	AGA AGC AGG CAT TGG AGA CAC C	543	81
	AAG CAG CCA CTT TGG GTT CC	251	
AβPP	CAA TCC AGG CAC AGA AAG AGT CC	478	96
	TTC CAT AAC CAA GAG AGG C	573	
GLUT4	GTA TCA TCT CTC AGT GGC TTG GAA G	394	111
	TTT CAT AGG AGG CAG CAG CG	504	
IDE	TGA TGA ATG ATG CCT GGA GAC TC	635	130
	TCA ATC CCT TCT TGG TTT GGT C	764	
18S	GGA CAC GGA CAG GAT TGA CA	1278	50
	ACC CAC GGA ATC GAG AAA GA	1327	
28S	GGT AAA CGG CGG GAG TAA CTA TG	3712	107
	TAG GTA GGG ACA GTG GGA ATC TCG	3818	

*IGF = insulin like growth factor; IRS = insulin receptor substrate; AβPP = amyloid β protein precursor; GLUT4 = glucose transporter 4; IDE = Insulin degrading enzyme.

Insulin and IGF-I receptors were expressed at significantly higher levels in control frontal cortex, hippocampus, and hypothalamus, than in corresponding regions of AD brains, whereas the mean levels of IGF-II receptor mRNA did not differ significantly between control and AD hippocampus and hypothalamus (Fig. 1). After re-plotting the insulin receptor data to highlight the regional and inter-group differences, it became evident that the mean levels of insulin and IGF-I receptor mRNA transcripts in the hippocampus and hypothalamus were 8- to 10-fold lower in AD than in corresponding regions of control brains, whereas in the frontal cortex, the inter-group differences, although significant, were much smaller as the insulin and IGF-I receptor mRNA transcript levels were reduced by approximately 40% in AD (Fig. 1A and 1D). Cerebellar tissue was analyzed because that brain region is regarded as relatively resistant to AD neurodegeneration. Correspondingly, the real time RT-PCR studies demonstrated similar mean levels of insulin, IGF-1, and IGF-II receptors in control and AD cerebellar tissue (Table 2).

3.3. *Reduced local growth factor expression in AD brains*

Real time quantitative RT-PCR studies detected insulin, IGF-I, and IGF-II polypeptide mRNA expression in aged control and AD brains. The highest growth factor expression was observed in the hippocampus and hypothalamus where the mean levels were 30- to 50-fold higher than in the frontal cortex (Fig. 2). Insulin gene expression was highest in the hippocampus, and undetectable in the frontal cortex. IGF-I mRNA expression was 10- to 30-fold higher in the hypothalamus than in the hippocampus or frontal cortex. IGF-II mRNA was expressed at similarly high levels in the hippocam-

Table 2
Growth factor and growth factor receptor expression in cerebellar cortex

RNA transcript	Control	Alzheimer	Significance
28S:18S Ratio	2.14 ± 0.56	2.28 ± 0.23	NS
Insulin receptor	1.92 ± 0.65 ($\times 10^{-5}$)	1.57 ± 0.98 ($\times 10^{-5}$)	NS
IGF-I receptor	1669.7 ± 174.7 ($\times 10^{-5}$)	1663.0 ± 627.1 ($\times 10^{-5}$)	NS
IGF-II receptor	170.2 ± 58.8 ($\times 10^{-5}$)	306.1 ± 146.3 ($\times 10^{-5}$)	NS
Insulin	4.54 ± 0.23 ($\times 10^{-5}$)	0.63 ± 0.29 ($\times 10^{-5}$)	$P = 0.01$
IGF-I	5810.6 ± 990.4 ($\times 10^{-5}$)	3845.2 ± 825.4 ($\times 10^{-5}$)*	NS
IGF-II	39.3 ± 3.49 ($\times 10^{-5}$)	26.7 ± 8.02 ($\times 10^{-5}$)	NS

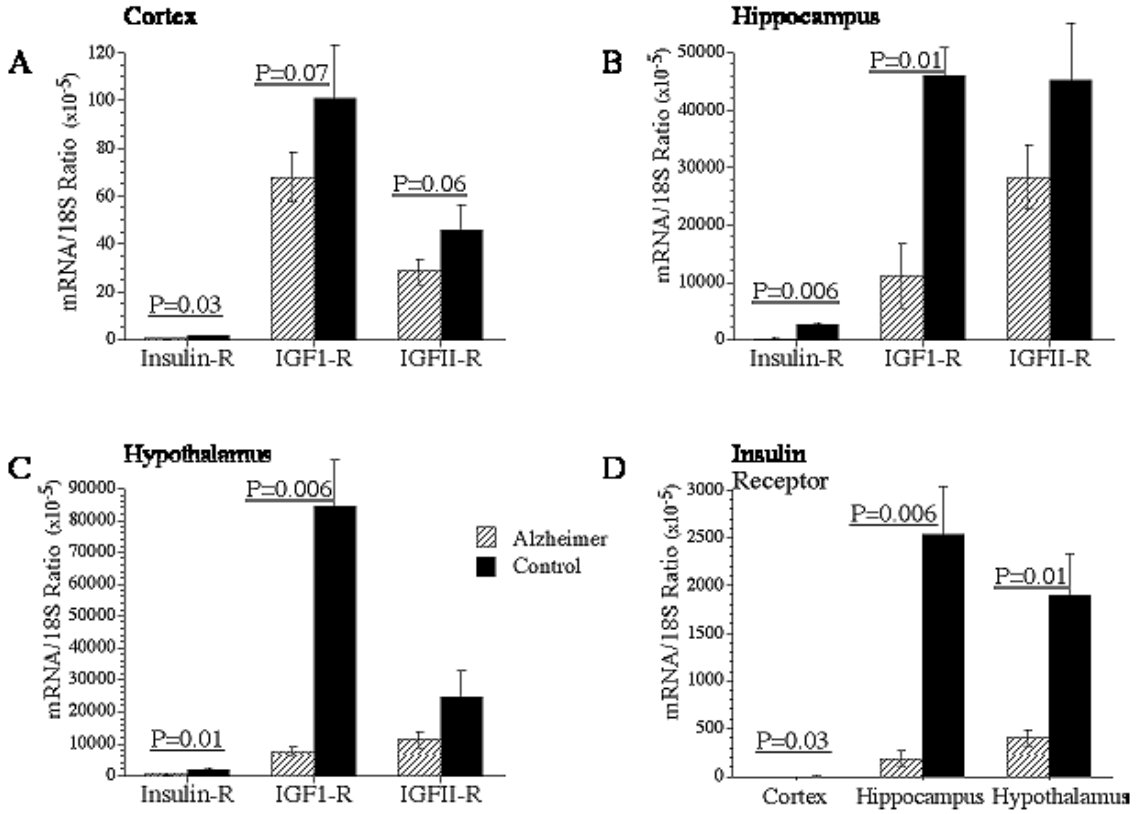

Fig. 1. Reduced levels of insulin, insulin-like growth factor, type I (IGF-I), and IGF-II receptor expression in AD brains demonstrated using real time quantitative RT-PCR. RNA was extracted from the frontal cortex, hippocampus, hypothalamus, and cerebellum (see Table 2) of AD and aged control snap frozen postmortem brain tissue. RNA was reverse transcribed using random primers. mRNA levels were measured using gene specific primers (Table 1), and the values were normalized to 18S ribosomal RNA. Graphs depict the mean $\pm$ S.E.M. of results obtained for the frontal cortex (A), hippocampus (B), and hypothalamus (C). (D) To better depict the inter-group and regional differences in insulin receptor expression, those data were re-graphed to scale. Data were analyzed statistically using repeated measures ANOVA with the post-hoc Tukey-Kramer significance test. Significant P-values (including trends) are indicated over the bar graphs.

pus and hypothalamus, and both were approximately 40-fold higher than in the frontal cortex. Re-analysis of the data by region demonstrated relatively high levels of insulin and IGF-II in the hippocampus, and IGF-II $>$ IGF-I$>>>$ insulin expression in the hypothalamus and frontal cortex (Fig. 2).

In AD, insulin gene expression in the hippocampus and hypothalamus was significantly reduced relative to control (insulin gene expression was not detected in the frontal cortex). Insulin mRNA expression was 4-fold lower in the hippocampus and 2-fold lower in the hypothalamus of AD relative to control brains. The mean levels of IGF-I mRNA expression in the AD hypothalamus and frontal cortex were 5- to 6-fold lower than in corresponding regions of control brains, whereas in the hippocampus, the mean levels of IGF-I expression

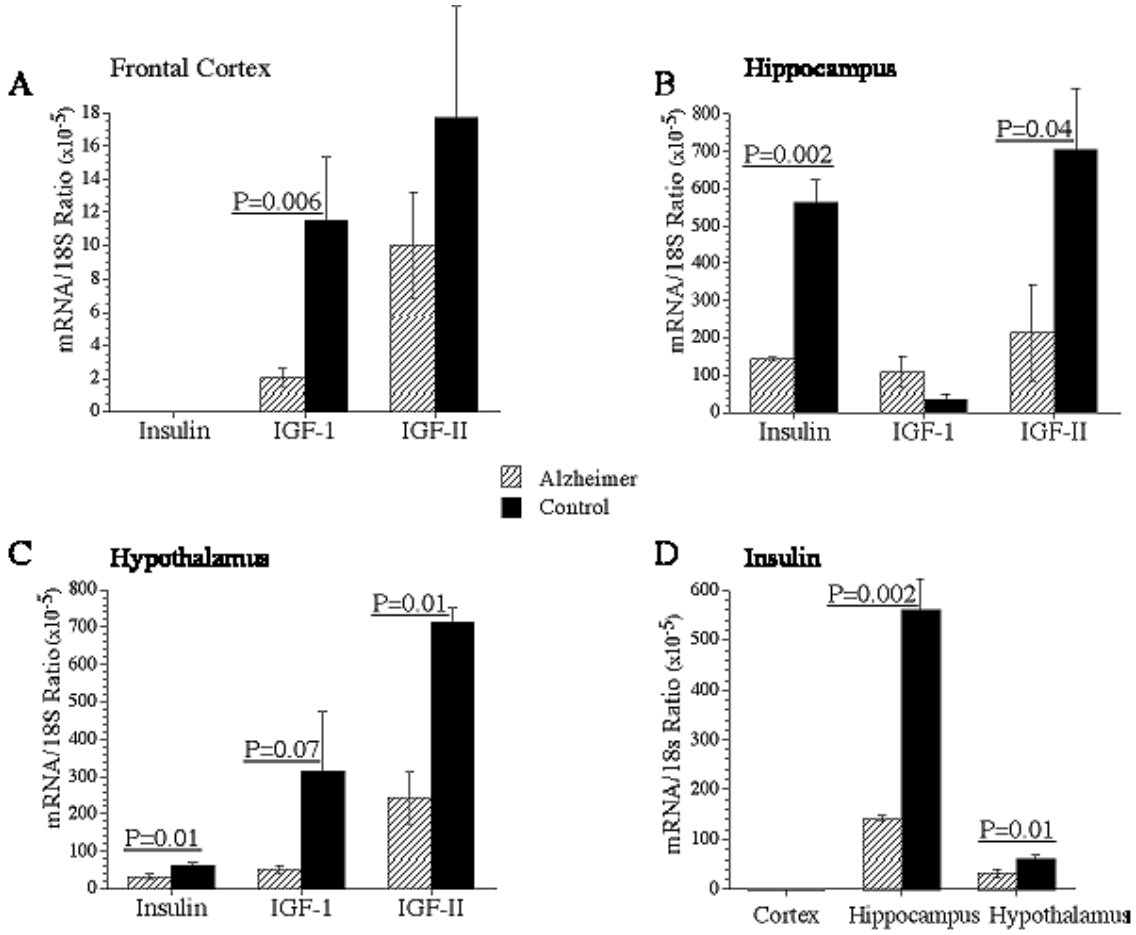

Fig. 2. Altered expression of insulin, IGF-I, and IGF-II in AD, demonstrated using real time quantitative RT-PCR as described in the legend to Fig. 1 (also see Methods). Graphs depict the mean ± S.E.M. of results obtained for the frontal cortex (A), hippocampus (B), and hypothalamus (C). To better depict the inter-group and regional differences in insulin gene expression, those data were re-graphed to scale (D). Data were analyzed statistically using repeated measures ANOVA with the post-hoc Tukey-Kramer significance test. Significant P-values (including trends) are indicated over the bar graphs.

did not significantly differ between the groups (Fig. 2). Finally, IGF-II mRNA levels were also significantly reduced (3-fold) in AD hippocampus and hypothalamus. In the frontal cortex, IGF-II expression was also reduced in AD, but the difference from control was relatively modest (∼35%) and did not reach statistical significance. In cerebellar tissue, insulin gene expression was significantly lower in AD relative to control cases ($P = 0.01$), and IGF-1 expression was also reduced, although the inter-group differences were not statistically significant (Table 2). In contrast, the IGF-II mRNA levels were similar in the AD and control cerebella. The significantly reduced levels of insulin gene expression found in AD cerebellar tissue suggest that insulin deficiency occurs globally in AD brains.

3.4. Reduced neuronal insulin, IGF-I, insulin receptor and IGF-I receptor immunoreactivity in AD brains

The cellular distributions of insulin, IGF-I, and the corresponding receptors were examined by immunohistochemical staining of formalin fixed, paraffin embedded sections of frontal cortex, hippocampus, and hypothalamus from 14 AD and 10 controls. Immunoreactivity corresponding to insulin or IGF-I polypeptides was observed in neurons and neuritic processes, whereas the insulin and IGF-I receptors were found expressed in neurons, neuropil neurites, glia, and smooth muscle cells of both parenchymal and leptomeningeal vessels. Insulin-, IGF-I-, insulin receptor-, and IGF-I receptor-positive neurons were less abundant in the AD

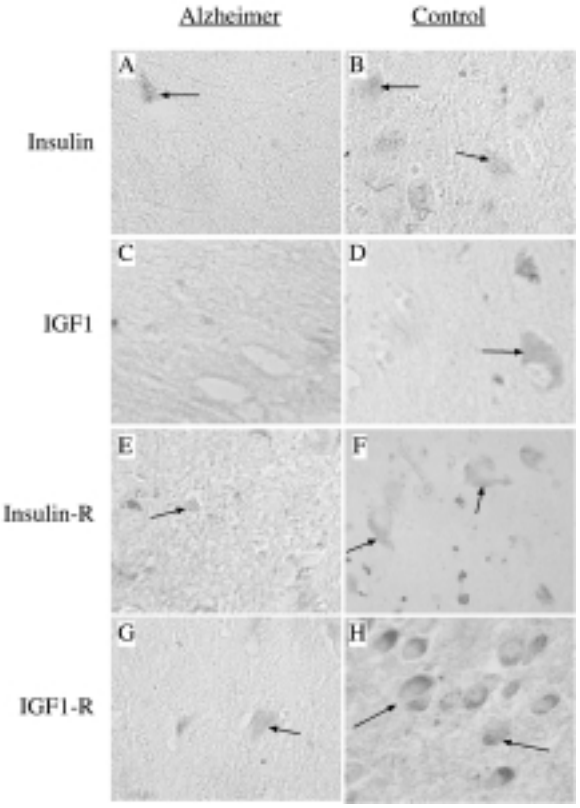

Fig. 3. Localization of insulin (A–B), IGF-I (C–D), insulin receptor (E–F), and IGF-I receptor (G–H) immunoreactivity in AD (A, C, E, G) and aged control (B, D, F, H) hippocampus using immunohistochemical staining. Formalin fixed paraffin embedded tissue sections were immunostained to detect growth factor and receptor expression by the Avidin-biotin horseradish peroxidase method using diaminobenzidine or NovaRed as the chromagen. The sections were counterstained with Hematoxylin. Arrows point to examples of labeled neurons.

compared with the normal aged control hippocampal samples (Fig. 3). Reduced neuronal labeling in the AD cases was attributable to loss of neurons as well as reduced neuronal expression of the growth factors and corresponding growth factor receptors. The latter was evident from the negative immunostaining reactions observed in histologically intact appearing neurons (Fig. 3). In contrast, the degrees of growth factor receptor labeling in vessels were similar in the AD and control samples (data not shown). For the most part, the findings by immunohistochemical staining corresponded with the results obtained by real time quantitative RT-PCR. The only exception was that IGF-I immunoreactivity was markedly reduced in AD hippocampal neurons, despite the similar mean mRNA levels detected in the homogenates.

3.5. Detection of insulin, IGF-I, IGF-II, and the corresponding receptor mRNA transcripts in primary neuronal cultures

To confirm the findings of neuronal growth factor and growth factor receptor expression in the CNS, investigations were extended by measuring the the same mRNA transcripts in cultured CNS neurons by real time quantitative RT-PCR using rat gene specific primers (Table 3). Primary neuronal cultures were generated from fetal rat cerebral cortex, hypothalamus, and hippocampus, and postnatal rat cerebellar granule neurons, as previously described [18,19,21,29,30]. At the time of harvesting, the neurons were post-mitotic and had abundant processes characteristic of differentiated cells. The real time quantitative RT-PCR studies demonstrated expression of insulin, IGF-I, IGF-II, insulin receptor, IGF-I receptor, and IGF-II receptor mRNA transcripts in cultured neurons (Figs 4 and 5). Insulin, IGF-I, and IGF-II receptors were expressed at strikingly higher levels in cerebellar granule neurons compared with neurons of cerebral origin (Fig. 4A–4C). Among the cerebral structures, insulin and IGF-II receptor mRNA levels were most abundantly expressed in cortical neurons, and at similarly lower levels in the hippocampus and hypothalamus (Fig. 4A–4C). IGF-1 receptor mRNA was abundantly expressed in cortical and hypothalamic neurons, where the mean levels were approximately 10-fold higher than in hippocampal neurons. Further analysis of the data to highlight the regional differences in growth factor receptor expression demonstrated that in the cerebellum, insulin receptor expression was most abundant, followed by IGF-I receptor, and then IGF-II receptor, whereas in cortical and hypothalamic neurons, the order of receptor abundance was IGF-I $>>$ IGF-II $>$ Insulin (Fig. 4D and 4E). In hippocampal neurons, IGF-II receptor mRNA was most abundant, followed by insulin receptor, and then IGF-I receptor.

Insulin polypeptide gene expression was most abundantly expressed in cortical neurons followed by cerebellar granule and hippocampal neurons. Hypothalamic neurons expressed the lowest levels of the insulin polypeptide mRNA (Fig. 5A). IGF-I and IGF-II polypeptide genes were expressed at significantly higher levels in cerebellar granule neurons compared with neurons isolated from the cerebral cortex, hippocampus, or hypothalamus (Fig. 5B and 5C). Among the cerebral structures, IGF-I was most abundantly expressed in cortical neurons, and at similarly lower levels in hippocampal and hypothalamic neurons (Fig. 5B,

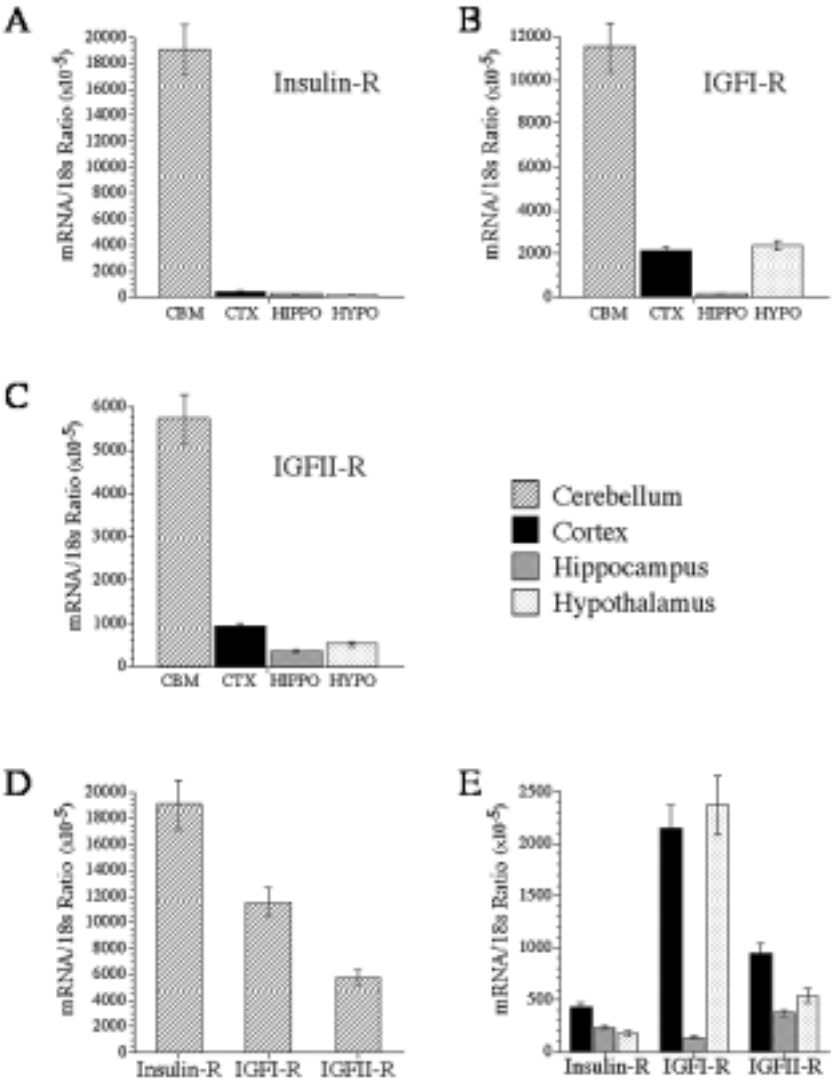

Fig. 4. Detection of insulin, IGF-I, and IGF-II receptor expression in post-mitotic differentiated primary neuronal cultures generated from rat postnatal cerebellar cortex (CBM), and rat fetal cerebral cortex (CTX), hippocampus (HIPPO), and hypothalamus (HYPO). Total RNA was extracted from the cultured cells and reverse transcribed using random oligodeoxynucleotide primers. mRNA levels were measured using gene specific primers (Table 3), and the values were normalized to 18S ribosomal RNA. Graphs depict the mean ± S.E.M. of results obtained for insulin receptor (A), IGF-I receptor (B), and IGF-II receptor (C) expression levels. To better depict the inter-group and regional differences in growth factor receptor expression, the data corresponding to cerebellar neurons (D) or cortical, hippocampal, and hypothalamic neurons (E) were re-graphed to scale.

5C and 5E). IGF-II polypeptide gene expression was highest in hippocampal neurons, followed by cortical, and then hypothalamic neurons (Fig. 5C and 5E). Further analysis of the regional differences in growth factor gene expression revealed that IGF-II was the most abundantly expressed growth factor in both cerebellar and cerebral neurons, while IGF-I was the next highest (Fig. 5D and 5E). Insulin mRNA levels were 1000- to 2500-fold lower than those of IGF-I or IGF-II in cerebellar granule neurons, and 10- to 50-fold lower than IGF-I or IGF-II in cortical and hippocampal neurons (Fig. 5D and 5E).

3.6. Analysis of critical insulin/IGF-I survival signaling mechanisms

Insulin and IGF-I mediate their effects by activating complex intracellular signaling pathways that are ini-

Table 3
Primer pairs for real time quantitative RT-PCR analysis of rat cultured neurons*

Primer	Sequence (5′–>3′)	Position (mRNA)	Amplicon size (bp)
Insulin	TTC TAC ACA CCC AAG TCC CGT C	189	134
	ATC CAC AAT GCC ACG CTT CTG C	322	
Insulin receptor	GGT AGA AAC CAT TAC TGG CTT CCT C	1037	125
	CGT AGA GAG TGT AGT TCC CAT CCA C	1161	
IGF-I	CAC TTC TTT CTA CAC AAC TCG GGC	1032	147
	CGA CTT GCT GCT GCT TTT GAG	1178	
IGF-I receptor	AGG GCG TAG TTG TAG AAG AGT TTC C	395	101
	TAC TTG CTG CTG TTC CGA GTG G	295	
IGF-II	CTG ATT GCT CTA CCC ACC CAA G	996	76
	TTG CTC ACT TCC GAT TGC TGG C	1071	
IGF-II receptor	CAC GAC TTG AAG ACA CGC ACT TAT C	403	132
	GCT GCT CTG GAC TCT GTG ATT TG	534	

tiated by ligand binding to the corresponding cell surface receptors, leading to autophosphorylation and activation of the intrinsic receptor tyrosine kinases [31–33]. Insulin/IGF-I receptor tyrosine kinases phosphorylate IRS molecules [32,34–36], which transmit signals downstream by activating the Erk MAPK and PI3 kinase/Akt pathways, and inhibit GSK-3β. Major responses to growth factor stimulated signaling through IRS molecules include increased cell growth and survival, and inhibition of apoptosis [36–43].

To examine the integrity of signaling pathways activated by insulin/IGF-I, we assessed the protein levels of the insulin and IGF-I receptors by Western blot analysis, and tyrosyl phosphorylated (PY) insulin and IGF-I receptors by immunoprecipitation/Western blot analysis (Fig. 6A–6D). IRS-1, IRS-2, and IRS-4 mRNA levels were measured using real time quantitative RT-PCR (Fig. 6E–6G). IRS-3 was not examined because that isoform is only expressed in rodent adipose tissue. Since one of the key signaling pathways activated by insulin/IGF-I signaling downstream through IRS is PI3 kinase-Akt, which is mediated by binding of the p85 subunit of PI3 kinase to a specific motif located within the carboxyl terminal region of IRS proteins [44], we investigated the integrity of this pathway in AD. This was accomplished by examining the degrees of interaction between the p85 subunit of PI3 kinase and PY-IRS by immunoprecipitation/Western blot analysis (Fig. 6H). The levels of Akt, phospho-Akt, GSK-3β, phospho-GSK-3β, and β-actin (control) were assessed by direct Western blot analysis with digital image densitometry (Fig. 7). In addition, *tau* and amyloid precursor protein mRNA levels were measured (Fig. 8A–8D) because both molecules are abnormally expressed or processed in AD, and previous studies demonstrated that *tau*, but not AβPP expression is regulated by insulin/IGF-I stimulation [45,46]. Analyses focused on the hippocampal and hypothalamic regions, given their relatively high levels of growth factor and growth factor receptor expression compared with the frontal cortex.

Corresponding with the real time quantitative RT-PCR results, IGF-I receptor protein levels were higher than insulin receptor levels, and both were expressed at significantly higher levels in control compared with AD samples (Fig. 6A and 6B). Correspondingly, the levels of PY-Insulin and PY-IGF-I receptors were significantly reduced in AD relative to control samples (Fig. 6C and 6D). Real time quantitative RT-PCR demonstrated significantly higher levels of IRS-1 compared with IRS-2 or IRS-4 mRNA transcripts ($P < 0.001$) in the frontal cortex, hippocampus, and hypothalamus (Fig. 6E–6G). IRS-4 was next in abundance, while IRS-2 was the least abundant of the IRS transcripts. In control brains, IRS-1 expression was approximately ten-fold higher in the hippocampus or hypothalamus compared with the frontal cortex. Similar trends were observed in AD, although the magnitude of the regional differences were not as striking. In the three brain regions examined, IRS-1 mRNA levels were significantly reduced in AD relative to control samples (Fig. 6E–6G). IRS-2 expression was also significantly reduced in AD hippocampus, but not in the other regions examined. IRS-4 mRNA transcripts were similarly abundant in AD and control brains. Immunoprecipitation/Western blot analysis demonstrated significantly reduced levels of p85-associated IRS-1 in AD relative to control hippocampal (Fig. 6H) and hypothalamic (data not shown) tissues, reflecting both reduced levels of IRS-1 expression and impaired signaling through IRS-1 molecules. IRS-2 and IRS-4 interactions with p85 were not pursued because these

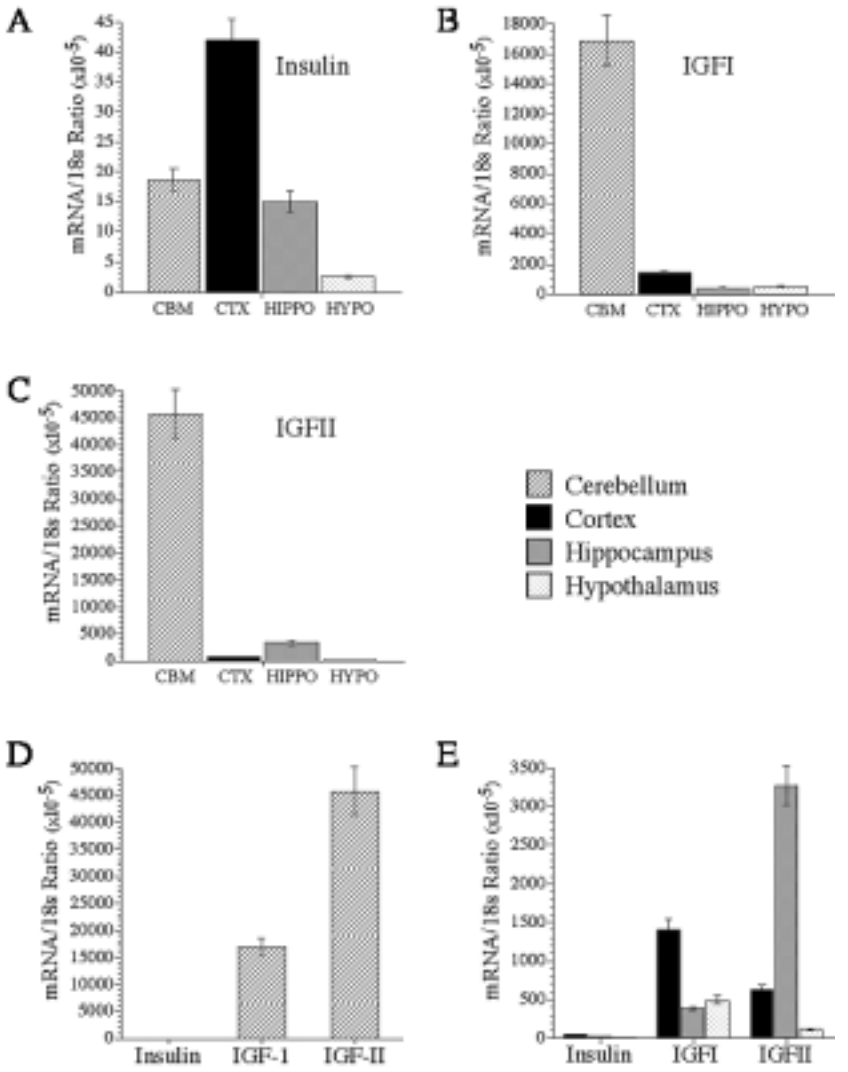

Fig. 5. Detection of insulin, IGF-I, and IGF-II gene expression in post-mitotic differentiated primary neuronal cultures generated from rat postnatal cerebellar cortex (CBM), and rat fetal cerebral cortex (CTX), hippocampus (HIPPO), and hypothalamus (HYPO). Total RNA was extracted from the cultured cells and reverse transcribed using random oligodeoxynucleotide primers. mRNA levels were measured using gene specific primers (Table 3), and the values were normalized to 18S ribosomal RNA. Graphs depict the mean ± S.E.M. of results obtained for insulin (A), IGF-I (B), and IGF-II (C) expression levels. To better depict the inter-group and regional differences in growth factor expression, the data corresponding to cerebellar neurons (D) or cortical, hippocampal, and hypothalamic neurons (E) were re-graphed to scale.

molecules were difficult to detect by Western blot analysis due to their low expression levels.

Further investigations of insulin and IGF-I stimulated survival signaling mechanisms were conducted using hippocampal and hypothalamic tissue samples due to their relatively high levels of growth factor and growth factor receptor expression compared with the frontal cortex. Survival signaling downstream of PI3 kinase is associated with increased levels of phospho-Akt and phospho-GSK-3β since phosphorylation leads to activation of Akt kinase and inhibition of GSK-3β activity. Western blot analysis with densitometry demonstrated significantly reduced mean levels of phospho-Akt (Fig. 7A) and phospho-GSK-3β (Fig. 7C) but similar mean levels of total Akt (Fig. 7B) and GSK-3β (Fig. 7D) in hippocampal tissue. Similar results were obtained using hypothalamic tissue samples (data not shown). The relatively reduced levels of phospho-Akt and phospho-GSK-3β reflect constitutively reduced levels of Akt kinase activity and increased levels of GSK-3β activity in AD. In contrast, β-actin expression

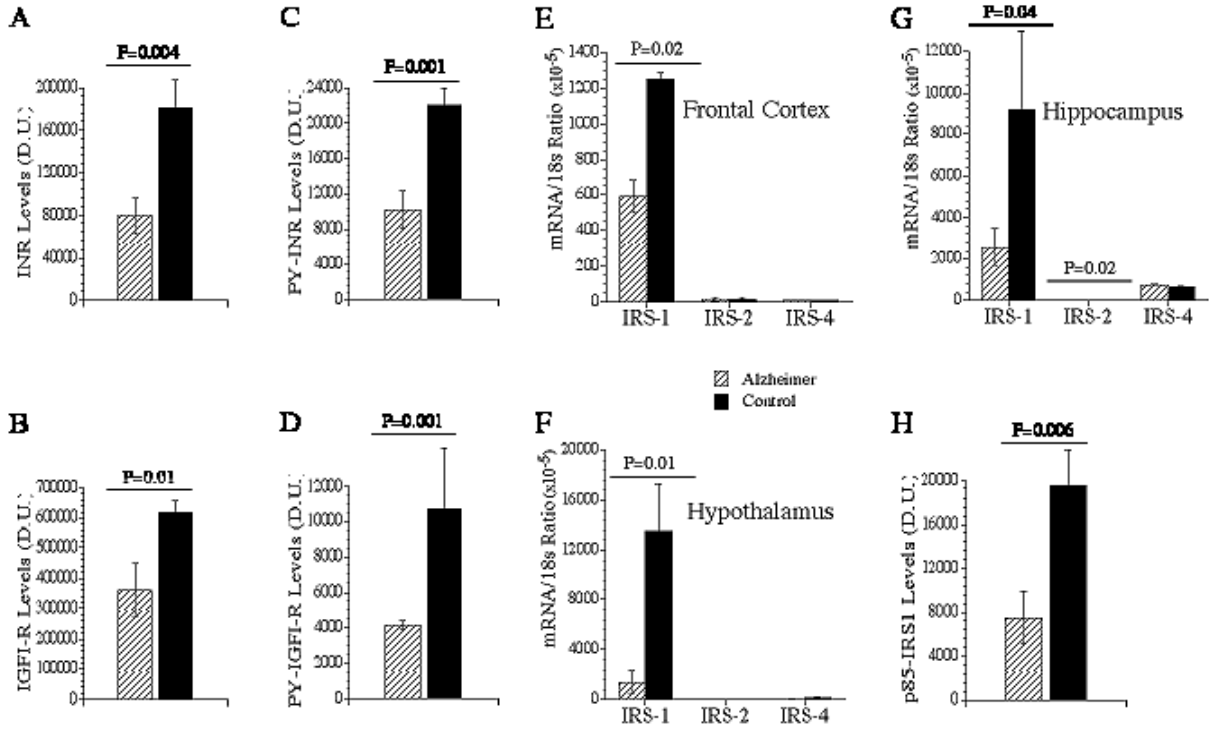

Fig. 6. Impaired insulin and IGF-I signaling mechanisms and reduced insulin receptor substrate, type 1 (IRS-1) expression in AD brains. Steady state levels of insulin receptor (A; INR) and IGF-I receptor (B; IGF-IR) protein expression were examined in hippocampal tissue samples by direct Western blot analysis. Tyrosine phosphorylated (PY) insulin receptor(C; PY-INR) and PY-IGF-IR (D) levels were assessed in hippocampal tissue samples by Western blot analysis of immunoprecipitates. IRS-1, IRS-2, and IRS-4 mRNA levels were measured in the frontal cortex (E), hippocampus (F), and hypothalamus (G) of AD and aged control brains using real time quantitative RT-PCR (See Methods) with values normalized to 18S RNA. Associations between the catalytically active p85 subunit of PI3 kinase and IRS-1 (reflecting PY-IRS-1-associated PI3 kinase activity) were evaluated in hippocampal tissue samples by Western blot analysis of immunoprecipitates (H). Immunoreactivity was revealed with horseradish peroxidase conjugated secondary antibody and enhanced chemiluminescence reagents. The levels of immunoreactivity were quantified by digital image densitometry (D.U.= arbitrary densitometry units). Data were analyzed statistically using Student t-tests or repeated measures ANOVA with the post-hoc Tukey-Kramer significance test. Significant P-values are indicated over the bar graphs.

was not significantly reduced in AD relative to aged control brains (Fig. 7E).

Since *tau* expression is regulated by insulin/IGF-I and Aβ turnover is mediated in part by insulin degrading enzyme (IDE), studies were conducted to measure the mRNA levels of *tau* and IDE. In addition, since glucose uptake and utilization are regulated in part by glucose transporter molecules, including GLUT4, and increased APP expression could account for Aβ accumulation in the brain, the real time RT-PCR studies were extended to measure the mRNA levels of GLUT4 and AβPP mRNA transcripts in hippocampal and hypothalamic tissues. Those studies demonstrated significantly reduced levels of *tau* and significantly increased levels of AβPP mRNA transcripts in AD relative to control cases (Fig. 8A–8D). In contrast, no significant differences in the mean levels of GLUT4 or IDE mRNA transcripts were observed between the AD and control cases (Fig. 8E–8H).

4. Discussion

4.1. Reduced growth factor receptor expression in AD

Using real time quantitative RT-PCR we detected significant reductions in insulin and IGF-I receptor expression levels in AD frontal cortex, hippocampus, and hypothalamus, but not in the cerebellum which is generally preserved in the context of AD neurodegeneration. IGF-II receptor expression was also significantly reduced in AD frontal cortex, and moderately, although not significantly reduced in AD hippocampus and hypothalamus. Further studies using immunohistochemical staining of postmortem brain tissue or real time quantitative RT-PCR analysis of cultured neurons, demonstrated that all three growth factor receptors were expressed in CNS neurons. The reduced expression levels of the insulin and IGF-I receptors could not be

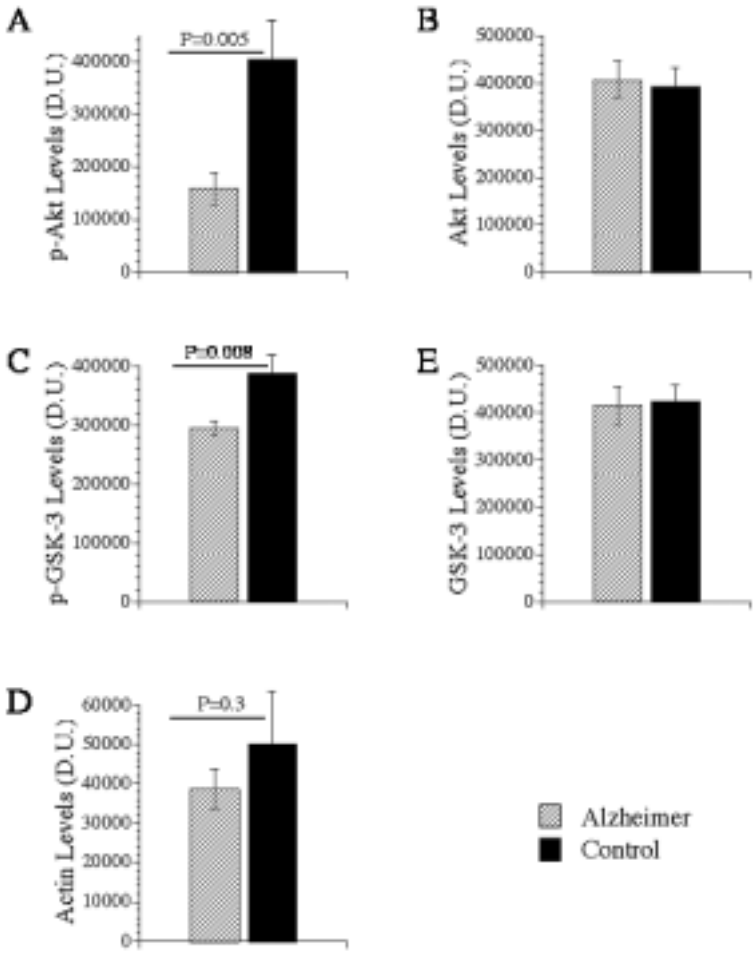

Fig. 7. Impaired survival signaling mechanisms in AD brains. Steady state levels of phospho-Akt (A; p-Akt; Thr308), total Akt (B), phospho-glycogen synthase kinase 3 (C; p-GSK-3α/β(Ser21/9)), total GSK-3 (D), and β-Actin (E) were assessed in hippocampal specimens by Western blot analysis. Phosphorylated proteins were detected using phospho-specific antibodies. Immunoreactivity was revealed with horseradish peroxidase conjugated secondary antibody and enhanced chemiluminescence reagents. The levels of immunoreactivity were quantified by digital image densitometry (D.U.= arbitrary densitometry units). Graphs depict the mean $\pm$ S.E.M. of results. Data were analyzed statistically using Student T-tests. The relevant P-values are indicated over the bar graphs.

explained solely on the basis of neuronal loss because many histologically intact neurons in AD brains exhibited low levels or absent immunoreactivity. Moreover, the hypothalamus, which does not manifes extensive cell loss or neurodegeneration until late in the course of disease, showed striking reductions in receptor mRNA expression and immunoreactivity in AD. Reduced levels of growth factor receptor expression could impair signaling, and effectively cause insulin/IGF-I resistance in the brain. Here, it is important to emphasize that the abnormalities in AD are not restricted to insulin signaling pathways, since they also clearly involve IGF-I and possibly IGF-II stimulated mechanisms. A second conclusion is that abnormalities in growth factor activated cascades exist at the receptor level, which may have future therapeutic implications.

4.2. Local growth factor expression in the CNS

The epidemiological data characterizing the roles of peripheral insulin levels and diabetes mellitus in relation to AD is weak and conflicting. However, a clear relationship has been established between impaired insulin signaling and neurodegeneration [10,11,19,47, 48]. These disparities led us to explore the possibility that insulin, IGF-I and IGF-II might be locally produced in the CNS, and that AD might be associated with reduced levels of growth factor gene expression

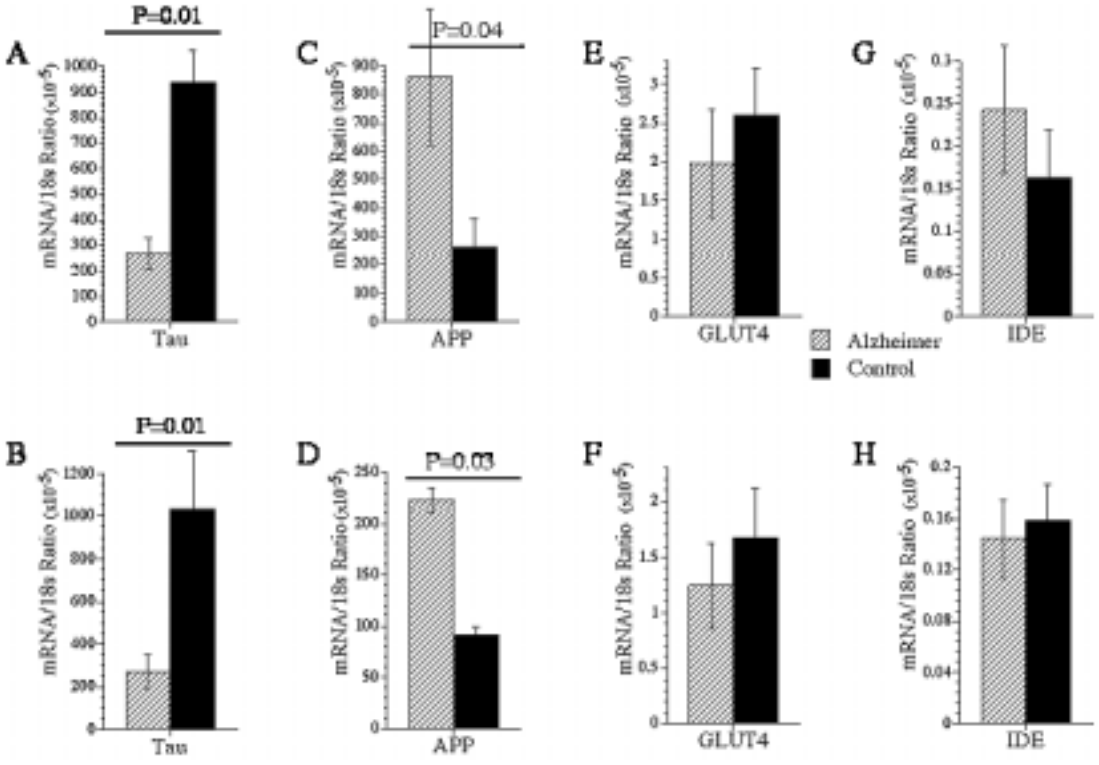

Fig. 8. Measurement of tau (A, B), amyloid β protein precursor (AβPP; C, D), glucose transporter 4 (GLUT4; E, F), and insulin degrading enzyme (IDE; G, H) mRNA expression in AD and control hippocampus (A, C, E, G) and hypothalamus (B, D, F, H) demonstrated using real time quantitative RT-PCR. Purified RNA was reverse transcribed using random primers. mRNA levels were measured using gene specific primers (Table 1) and the values were normalized to 18S ribosomal RNA. Graphs depict the mean $\pm$ S.E.M. of results. Data were analyzed statistically using Student t-tests. Significant P-values are indicated over the bar graphs.

in the brain. In addition to delineating a novel mechanism of AD-type neurodegeneration, the demonstration of CNS neuronal insulin and IGF-I expression could explain the unique ability of CNS neurons to take up glucose in an apparently insulin-independent fashion. To demonstrate local production of insulin, IGF-I, and IGF-II, it was necessary to detect the mRNA transcripts, since proteins or immunoreactivity could reflect transport and up-take from peripheral blood.

Real time quantitative RT-PCR studies demonstrated mRNA transcripts corresponding to insulin, IGF-I, and IGF-II in both aged control and AD brains. In normal aged brains, relatively high levels of insulin were detected in the hippocampus, and in general, growth factor expression was at least 10-fold higher in the hippocampus and hypothalamus than in the frontal cortex. Since both the hypothalamus and hippocampus are physically located close to a ventricle, the disproportionately high levels of insulin, IGF-I, and IGF-II expression in these structures may be important for regulating the distribution of growth factors to different brain regions, such as the frontal cortex where insulin gene expression was not detected and IGF-I and IGF-II gene expression were low-level. Neuronal expression of these growth factors was further confirmed by performing real time RT-PCR analysis of primary neuronal cultures generated from rat hippocampus, hypothalamus, cerebral cortex, and cerebellum. The finding of 100-fold or higher levels of growth factor expression in cerebellar granule neurons relative to the other neuronal subtypes is of interest because in rodents, the cerebellum develops much later than the cerebrum and cerebellar neurons remain mitotically active until 7–8 days after birth. The high levels of both growth factor and growth factor receptor gene expression may reflect autocrine or paracrine stimulation of cerebellar growth and development.

4.3. Reduced levels of growth factor gene expression in AD

Significantly reduced levels of insulin and IGF II gene expression were detected in the hippocampus and hypothalamus, and reduced IGF-I expression was

observed in the frontal cortex and hypothalamus in AD. Therefore, in AD, the problem is not simply insulin/IGF-I resistance since there is also a significant deficiency in local CNS growth factor production. Moreover, the additional finding of significantly lower levels of insulin peptide gene expression in AD cerebellum suggests that CNS insulin deficiency extends beyond structures that are particularly vulnerable to AD-type neurodegeneration. A paucity of local growth factor gene expression could substantially impair growth factor signaling in the CNS. Moreover, if the CNS were dependent on local growth factor production, reduced supply would produce a state of growth factor withdrawal, which is a well established mechanism of neuronal death. In order to maintain the integrity of insulin/IGF-I-dependent CNS functions, either the receptor sensitivity or expression levels must be increased, or a mechanism for increasing CNS uptake of growth factors from peripheral blood must be activated or enhanced. Further research is needed to determine the optimum means of bolstering insulin, IGF-I, and IGF-II expression and up-take in the CNS as a potential approach for preventing neurodegeneration. It should be emphasized that: 1) the problem in AD is not just insulin resistance since related growth factor gene expression is also diminished; 2) the insulin, IGF-I, and possibly IGF-II resistances stem from problems related to impaired CNS growth factor production, and either down-regulation of the corresponding receptors or progressive loss of neurons that bear those receptors; and 3) the finding that growth factor genes are expressed in CNS neurons raises questions and concerns about the potential benefits of peripherally administered replacement therapy.

4.4. Reduced neuronal insulin, IGF-I, insulin receptor and IGF-I receptor immunoreactivity in AD brains

The immunohistochemical staining studies demonstrated expression of both the growth factors and growth factor receptors in CNS neurons. These observations were validated by demonstrating growth factor receptor and growth factor gene expression in cultured neurons. Although growth factor immunoreactivity was mainly identified in neurons, other cell types including glia also expressed these same growth factors, as well as the corresponding receptors. One potential explanation for the shift in growth factor and receptor expression profiles observed in AD is that the neurodegeneration is accompanied by neuronal loss and glial cell activation. Insulin and IGF-I receptor expression was detected in the vasculature, as well as in choroid plexus epithelial cells, neurons, and glia. Insulin/IGF-I receptor expression in the vasculature has been previously reported, and suggests that CNS vessels may be responsive to changes in the circulating levels of these growth factor. There were no obvious differences between the AD and control groups with respect to growth factor receptor expression in vessels, suggesting that alterations in peripheral blood levels of insulin or IGF-I may not adversely affect CNS function to a greater extent in AD than in normal aging. Instead, local endogenous production may be most relevant with regard to growth factor regulation of CNS neuronal functions.

4.5. Analysis of key signaling molecules downstream of the insulin/IGF-I receptors

Insulin and IGF-I mediate their effects by activating complex intracellular signaling pathways initiated by ligand binding to cell surface receptors and attendant activation of intrinsic receptor tyrosine kinases [31–33]. Insulin/IGF-I receptor tyrosine kinases phosphorylate IRS molecules [32,34–36]. Tyrosyl phosphorylated IRS-1 (PY-IRS-1) transmits intracellular signals that mediate growth, metabolic functions, and survival by interacting with downstream src-homology 2 (SH2)-containing molecules through specific motifs located in the C-terminal region of IRS-1, with attendant activation of Erk MAPK and PI3 kinase/Akt, and inhibition of GSK-3β [44]. In this regard, binding of PY-IRS-1 to p85 stimulates glucose transport, and inhibits apoptosis by activating Akt/Protein kinase B or inhibiting GSK-3β [40–43,49]. Akt kinase inhibits apoptosis by phosphorylating GSK-3β and BAD, rendering them inactive [43,50–52]. Low levels of Akt kinase, and high levels of GSK-3β activity or activated BAD are associated with increased apoptosis and mitochondrial dysfunction in neuronal cells. BAD disrupts mitochondrial membrane permeability and promotes cytochrome c release, which activates caspases [51,52]. Perturbations in mitochondrial membrane permeability may increase cellular free radicals that cause mitochondrial DNA damage, impair mitochondrial function, and activate pro-apoptosis cascades [53,54].

The studies demonstrated that IRS-1 mRNA was more abundantly expressed than IRS-2 or IRS-4, and that in AD, the levels of IRS-1 mRNA were significantly reduced relative to normal aging. Although the mechanism of reduced IRS-1 expression is not known, exploratory studies in neuronal cell lines demonstrated

that IRS-1 expression is regulated by insulin and IGF-I stimulation (Carter, et al., 2004, Unpublished). The markedly reduced levels of IRS-1 gene expression are reminiscent of the murine IRS-1 and insulin receptor knock-out models which exhibit reduced brain and body weight due to impaired insulin stimulated growth and survival signaling [10,55,56]. In addition, humans with Type 2 diabetes and Syndrome X have significantly reduced levels of IRS-1 expression that is associated with impaired insulin signaling downstream through PI3 kinase and Akt [57].

Since insulin and IGF-I transmit pro-survival and pro-growth signaling through IRS molecules, the reduced levels of IRS expression could contribute to growth factor resistance in the CNS. Corresponding with the reduced levels of growth factor, growth factor receptor, and IRS gene expression, further analysis of the downstream signaling pathways demonstrated reduced level of IRS-associated PI3 kinase activity (reflected by reduced levels of p85-associated IRS-1), decreased levels of phospho-Akt (reflecting decreased Akt activity), and reduced levels of phospho-GSK-3β (reflecting increased GSK-3β activity). Therefore, the impaired growth factor and receptor expression were associated with constitutive inhibition survival signaling mechanisms in AD. The finding of reduced phospho-Akt contrasts with previous reports demonstrating increased phospho-Akt or Akt activity in AD brain tissue [58]. However, the latter result may reflect increased levels of oxidative stress in the tissue samples, rather than impaired insulin or IGF-1 signaling. The explanation is that Akt, as well as other pro-growth and stress kinases that have been shown by others to be increased in AD [59] can be activated by oxidative injury [60–63], and in that context, chemical inhibition of growth or stress kinases may provide neuroprotection [64].

The reduced *tau* expression observed in AD is of interest because previous studies demonstrated that neuronal *tau* mRNA expression was regulated by IGF-I and insulin stimulation [45]. Therefore, the AD-associated reductions in *tau* mRNA correlate with the impaired insulin and IGF-I signaling mechanisms observed in the same AD samples. Moreover, the increased levels of phospho-*tau* that are generally detected in AD brains could reflect impaired insulin/IGF-I signaling with attendant increased levels of GSK-3β activity, since GSK-3β is one of the major kinases responsible for hyper-phosphorylating *tau* [46]. The increased APP mRNA expression detected in AD brains is of further interest because the finding suggests a transcription-based mechanism for increased amyloid-β deposition in the brain. Increased APP expression due to higher levels of the corresponding transcript would provide more substrate and increased probability of aberrant cleavage and processing of the protein. The findings herein are also consistent with previous demonstrations that AβPP expression is increased with oxidative stress [29], and that increased levels of amyloid-β can be neurotoxic [65–67]. Impaired insulin signaling has already been linked to increased oxidative stress and mitochondrial dysfunction in neuronal cells [19,47,48]. Additional studies demonstrated that the AD-associated abnormalities in insulin/IGF-I signaling mechanisms were not accompanied by reduced expression of GLUT4 or IDE. Altogether, the results suggest that impaired insulin/IGF-I stimulated survival signaling and attendant chronic oxidative stress represent major abnormalities in AD. From the standpoint of therapeutic intervention, treatment with ligands that specifically enhance insulin/IGF-I signaling mechanisms may help to improve viability and function of neuronal cells at risk for AD-type neurodegeneration.

Acknowledgements

Supported by Grants AA12458, AA02666, and AA11931 from the National Institute of Alcoholism and Alcohol Abuse, and COBRE Award P20RR15578 from the National Institutes of Health.

References

[1] S. Hoyer, Glucose metabolism and insulin receptor signal transduction in Alzheimer disease, *Eur J Pharmacol* **490** (2004), 115–125.

[2] S. Hoyer, Causes and consequences of disturbances of cerebral glucose metabolism in sporadic Alzheimer disease: therapeutic implications, *Adv Exp Med Biol* **541** (2004), 135–152.

[3] S. Craft, S. Asthana, D.G. Cook, L.D. Baker, M. Cherrier, K. Purganan, C. Wait, A. Petrova, S. Latendresse, G.S. Watson, J.W. Newcomer, G.D. Schellenberg and A.J. Krohn, Insulin dose-response effects on memory and plasma amyloid precursor protein in Alzheimer's disease: interactions with apolipoprotein E genotype, *Psychoneuroendocrinology* **28** (2003), 809–822.

[4] S. Craft, S. Asthana, G. Schellenberg, L. Baker, M. Cherrier, A.A. Boyt, R.N. Martins, M. Raskind, E. Peskind and S. Plymate, Insulin effects on glucose metabolism, memory, and plasma amyloid precursor protein in Alzheimer's disease differ according to apolipoprotein-E genotype, *Ann N Y Acad Sci* **903** (2000), 222–228.

[5] C. Messier, Diabetes, Alzheimer's disease and apolipoprotein genotype, *Exp Gerontol* **38** (2003), 941–946.

[6] S. Hoyer, The brain insulin signal transduction system and sporadic (type II) Alzheimer disease: an update, *J Neural Transm* **109** (2002), 341–360.
[7] J.R. McDermott and A.M. Gibson, Degradation of Alzheimer's beta-amyloid protein by human and rat brain peptidases: involvement of insulin-degrading enzyme, *Neurochem Res* **22** (1997), 49–56.
[8] W.Q. Qiu, D.M. Walsh, Z. Ye, K. Vekrellis, J. Zhang, M.B. Podlisny, M.R. Rosner, A. Safavi, L.B. Hersh and D.J. Selkoe, Insulin-degrading enzyme regulates extracellular levels of amyloid beta-protein by degradation, *J Biol Chem* **273** (1998), 32730–32738.
[9] W. Farris, S. Mansourian, M.A. Leissring, E.A. Eckman, L. Bertram, C.B. Eckman, R.E. Tanzi and D.J. Selkoe, Partial loss-of-function mutations in insulin-degrading enzyme that induce diabetes also impair degradation of amyloid beta-protein, *Am J Pathol* **164** (2004), 1425–1434.
[10] M. Schubert, D.P. Brazil, D.J. Burks, J.A. Kushner, J. Ye, C.L. Flint, J. Farhang-Fallah, P. Dikkes, X.M. Warot, C. Rio, G. Corfas and M.F. White, Insulin receptor substrate-2 deficiency impairs brain growth and promotes tauphosphorylation, *J Neurosci* **23** (2003), 7084–7092.
[11] M. Schubert, D. Gautam, D. Surjo, K. Ueki, S. Baudler, D. Schubert, T. Kondo, J. Alber, N. Galldiks, E. Kustermann, S. Arndt, A.H. Jacobs, W. Krone, C.R. Kahn and J.C. Bruning, Role for neuronal insulin resistance in neurodegenerative diseases, *Proc Natl Acad Sci USA* **101** (2004), 3100–3105.
[12] M.F. Beal, G. Uhl, M.F. Mazurek, N. Kowall and J.B. Martin, Somatostatin: alterations in the central nervous system in neurological diseases, *Res Publ Assoc Res Nerv Ment Dis* **64** (1986), 215–257.
[13] J.C. Reubi and J. Palacios, Somatostatin and Alzheimer's disease: a hypothesis, *J Neurol* **233** (1986), 370–372.
[14] M. Fisman, B. Gordon, V. Feleki, E. Helmes, T. McDonald and J. Dupre, Metabolic changes in Alzheimer's disease, *J Am Geriatr Soc* **36** (1988), 298–300.
[15] S. Hoyer, Somatostatin and Alzheimer's disease, *J Neurol* **234** (1987), 266–267.
[16] A. Tham, K. Sparring, D. Bowen, L. Wetterberg and V.R. Sara, Insulin-like growth factors and somatomedin B in the cerebrospinal fluid of patients with dementia of the Alzheimer type, *Acta Psychiatr Scand* **77** (1988), 719–723.
[17] G. Bucht, R. Adolfsson, F. Lithner and B. Winblad, Changes in blood glucose and insulin secretion in patients with senile dementia of Alzheimer type, *Acta Med Scand* **213** (1983), 387–392.
[18] S.M. de la Monte, T.R. Neely, J. Cannon and J.R. Wands, Ethanol impairs insulin-stimulated mitochondrial function in cerebellar granule neurons, *Cell Mol Life Sci* **58** (2001), 1950–1960.
[19] S.M. de la Monte and J.R. Wands, Chronic gestational exposure to ethanol impairs insulin-stimulated survival and mitochondrial function in cerebellar neurons, *CMLS, Cell Mol Life Sci* **59** (2002), 882–893.
[20] S.M. de la Monte, N. Ganju, K. Banerjee, N.V. Brown, T. Luong and J.R. Wands, Partial rescue of ethanol-induced neuronal apoptosis by growth factor activation of phosphoinositol-3-kinase, *Alcohol Clin Exp Res* **24** (2000), 716–726.
[21] J. Xu, J. Eun Yeon, H. Chang, G. Tison, G. Jun Chen, J.R. Wands and S.M. De La Monte, Ethanol impairs insulin-stimulated neuronal survival in the developing brain: Role of PTEN phosphatase, *J Biol Chem* **278** (2003), 26929–26937.
[22] H. Braak and E. Braak, Diagnostic criteria for neuropathologic assessment of Alzheimer's disease, *Neurobiol Aging* **18** (1997), S85–S88.
[23] Z. Nagy, D.M. Yilmazer-Hanke, H. Braak, E. Braak, C. Schultz and J. Hanke, Assessment of the pathological stages of Alzheimer's disease in thin paraffin sections: a comparative study, *Dement Geriatr Cogn Disord* **9** (1998), 140–144.
[24] J.E. Yeon, S. Califano, J. Xu, J.R. Wands and S.M. De La Monte, Potential role of PTEN phosphatase in ethanol-impaired survival signaling in the liver, *Hepatology* **38** (2003), 703–714.
[25] F. Ausubel, R. Brent, R. Kingston, D. Moore, J. Seidman, J. Smnith and K. Struhl, eds, *Current Protocols in Molecular Biology*, (2000).
[26] S.M. de la Monte, T. Luong, T.R. Neely, D. Robinson and J.R. Wands, Mitochondrial DNA damage as a mechanism of cell loss in Alzheimer's disease, *Lab Invest* **80** (2000), 1323–1335.
[27] S.L. Payao, M.A. Smith, L.M. Winter and P.H. Bertolucci, Ribosomal RNA in Alzheimer's disease and aging, *Mech Ageing Dev* **105** (1998), 265–272.
[28] A.M. da Silva, S.L. Payao, B. Borsatto, P.H. Bertolucci and M.A. Smith, Quantitative evaluation of the rRNA in Alzheimer's disease, *Mech Ageing Dev* **120** (2000), 57–64.
[29] G.J. Chen, J. Xu, S.A. Lahousse, N.L. Caggiano and S.M. de la Monte, Transient hypoxia causes Alzheimer-type molecular and biochemical abnormalities in cortical neurons: potential strategies for neuroprotection, *J Alzheimers Dis* **5** (2003), 209–228.
[30] E.A. Nillni, L.G. Luo, I.M. Jackson and P. McMillan, Identification of the thyrotropin-releasing hormone precursor, its processing products, and its coexpression with convertase 1 in primary cultures of hypothalamic neurons: anatomic distribution of PC1 and PC2, *Endocrinology* **137** (1996), 5651–5661.
[31] A. Ullrich, J.R. Bell, E.Y. Chen, R. Herrera, L.M. Petruzzelli, T.J. Dull, A. Gray, L. Coussens, Y.C. Liao and M. Tsubokawa, Human insulin receptor and its relationship to the tyrosine kinase family of oncogenes, *Nature* **313** (1985), 756–761.
[32] M.G. Myers, X.J. Sun and M.F. White, The IRS-1 signaling system, *Trends Biochem Sci* **19** (1994), 289–293.
[33] T. O'Hare and P.F. Pilch, Intrinsic kinase activity of the insulin receptor, *Int J Biochem* **22** (1990), 315–324.
[34] X.J. Sun, P. Rothenberg, C.R. Kahn, J.M. Backer, E. Araki, P.A. Wilden, D.A. Cahill, B.J. Goldstein and M.F. White, Structure of the insulin receptor substrate IRS-1 defines a unique signal transduction protein, *Nature* **352** (1991), 73–77.
[35] M.F. White, R. Maron and C.R. Kahn, Insulin rapidly stimulates tyrosine phosphorylation of a Mr-185,000 protein in intact cells, *Nature* **318** (1985), 183–186.
[36] X.J. Sun, D.L. Crimmins, M.J. Myers, M. Miralpeix and M.F. White, Pleiotropic insulin signals are engaged by multisite phosphorylation of IRS-1, *Mol Cell Biol* **13** (1993), 7418–7428.
[37] D.G. Puro and E. Agardh, Insulin-mediated regulation of neuronal maturation, *Science* **225** (1984), 1170–1172.
[38] J.F. Mill, M.V. Chao and D.N. Ishii, Insulin, insulin-like growth factor II, and nerve growth factor effects on tubulin mRNA levels and neurite formation, *Proc Natl Acad Sci USA* **82** (1985), 7126–7130.
[39] K. Lam, C.L. Carpenter, N.B. Ruderman, J.C. Friel and K.L. Kelly, The phosphatidylinositol 3-kinase serine kinase phosphorylates IRS-1. Stimulation by insulin and inhibition by Wortmannin, *J Biol Chem* **269** (1994), 20648–20652.

[40] G. Kulik, A. Klippel and M.J. Weber, Antiapoptotic signalling by the insulin-like growth factor I receptor, phosphatidylinositol 3-kinase, and Akt, *Mol Cell Biol* **17** (1997), 1595–1606.
[41] H. Dudek, S.R. Datta, T.F. Franke, M.J. Birnbaum, R. Yao, G.M. Cooper, R.A. Segal, D.R. Kaplan and M.E. Greenberg, Regulation of neuronal survival by the serine-threonine protein kinase Akt, *Science* **275** (1997), 661–665.
[42] B.M. Burgering and P.J. Coffer, Protein kinase B (c-Akt) in phosphatidylinositol-3-OH kinase signal transduction, *Nature* **376** (1995), 599–602.
[43] M. Delcommenne, C. Tan, V. Gray, L. Rue, J. Woodgett and S. Dedhar, Phosphoinositide-3-OH kinase-dependent regulation of glycogen synthase kinase 3 and protein kinase B/AKT by the integrin-linked kinase, *Proc Natl Acad Sci USA* **95** (1998), 11211–11216.
[44] B. Giovannone, M.L. Scaldaferri, M. Federici, O. Porzio, D. Lauro, A. Fusco, P. Sbraccia, P. Borboni, R. Lauro and G. Sesti, Insulin receptor substrate (IRS) transduction system: distinct and overlapping signaling potential, *Diabetes Metab Res Rev* **16** (2000), 434–441.
[45] S.M. de la Monte, G.J. Chen, E. Rivera and J.R. Wands, Neuronal thread protein regulation and interaction with microtubule-associated proteins in SH-Sy5y neuronal cells, *Cell Mol Life Sci* **60** (2003), 2679–2691.
[46] M. Hong and V.M. Lee, Insulin and insulin-like growth factor-1 regulate tauphosphorylation in cultured human neurons, *J Biol Chem* **272** (1997), 19547–19553.
[47] S. Hoyer, S.K. Lee, T. Loffler and R. Schliebs, Inhibition of the neuronal insulin receptor, An in vivo model for sporadic Alzheimer disease? *Ann N Y Acad Sci* **920** (2000), 256–258.
[48] S. Hoyer and H. Lannert, Inhibition of the neuronal insulin receptor causes Alzheimer-like disturbances in oxidative/energy brain metabolism and in behavior in adult rats, *Ann N Y Acad Sci* **893** (1999), 301–303.
[49] Y. Kido, J. Nakae and D. Accili, Clinical review 125: The insulin receptor and its cellular targets, *J Clin Endocrinol Metab* **86** (2001), 972–979.
[50] S.R. Datta, H. Dudek, X. Tao, S. Masters, H. Fu, Y. Gotoh and M.E. Greenberg, Akt phosphorylation of BAD couples survival signals to the cell intrinsic death machinery, *Cell* **91** (1997), 231–241.
[51] S.G. Kennedy, E.S. Kandel, T.K. Cross and N. Hay, Akt/Protein kinase B inhibits cell death by preventing the release of cytochrome c from mitochondria, *Mol Cell Biol* **19** (1999), 5800–5810.
[52] A. Brunet, A. Bonni, M.J. Zigmond, M.Z. Lin, P. Juo, L.S. Hu, M.J. Anderson, K.C. Arden, J. Blenis and M.E. Greenberg, Akt promotes cell survival by phosphorylating and inhibiting a Forkhead transcription factor, *Cell* **96** (1999), 857–868.
[53] H. Jaeschke, G.J. Gores, A.I. Cederbaum, J.A. Hinson, D. Pessayre and J.J. Lemasters, Mechanisms of hepatotoxicity, *Toxicol Sci* **65** (2002), 166–176.
[54] J.G. Pastorino, S.T. Chen, M. Tafani, J.W. Snyder and J.L. Farber, The overexpression of Bax produces cell death upon induction of the mitochondrial permeability transition, *J Biol Chem* **273** (1998), 7770–7775.
[55] S. Doublier, C. Duyckaerts, D. Seurin and M. Binoux, Impaired brain development and hydrocephalus in a line of transgenic mice with liver-specific expression of human insulin-like growth factor binding protein-1, *Growth Horm IGF Res* **10** (2000), 267–274.
[56] T. Nishiyama, T. Shirotani, T. Murakami, F. Shimada, M. Todaka, S. Saito, H. Hayashi, Y. Noma, K. Shima, H. Makino et al., Expression of the gene encoding the tyrosine kinase-deficient human insulin receptor in transgenic mice, *Gene* **141** (1994), 187–192.
[57] U. Smith, M. Axelsen, E. Carvalho, B. Eliasson, P.A. Jansson and C. Wesslau, Insulin signaling and action in fat cells: associations with insulin resistance and type 2 diabetes, *Ann N Y Acad Sci* **892** (1999), 119–126.
[58] A. Rickle, N. Bogdanovic, I. Volkman, B. Winblad, R. Ravid and R.F. Cowburn, Akt activity in Alzheimer's disease and other neurodegenerative disorders, *Neuroreport* **15** (2004), 955–959.
[59] X. Zhu, H.G. Lee, A.K. Raina, G. Perry and M.A. Smith, The role of mitogen-activated protein kinase pathways in Alzheimer's disease, *Neurosignals* **11** (2002), 270–281.
[60] S.M. de La Monte, N. Ganju, N. Feroz, T. Luong, K. Banerjee, J. Cannon and J.R. Wands, Oxygen Fre e Radical Injury Is Sufficient to Cause Some Alzheimer-Type Molecular Abnormalities in Human CNS Neuronal Cells, *J Alzheimers Dis* **2** (2000), 261–281.
[61] P. Kelicen, I. Cantuti-Castelvetri, C. Pekiner and K.E. Paulson, The spin trapping agent PBN stimulates H_2 O_2 -induced Erk and Src kinase activity in human neuroblastoma cells, *Neuroreport* **13** (2002), 1057–1061.
[62] A.J. Crossthwaite, S. Hasan and R.J. Williams, Hydrogen peroxide-mediated phosphorylation of ERK1/2, Akt/PKB and JNK in cortical neurones: dependence on Ca(2+) and PI3-kinase, *J Neurochem* **80** (2002), 24–35.
[63] H.J. Lin, X. Wang, K.M. Shaffer, C.Y. Sasaki and W. Ma, Characterization of H_2O_2-induced acute apoptosis in cultured neural stem/progenitor cells, *FEBS Lett* **570** (2004), 102–106.
[64] P.C. Chin, L. Liu, B.E. Morrison, A. Siddiq, R.R. Ratan, T. Bottiglieri and S.R. D'Mello, The c-Raf inhibitor GW5074 provides neuroprotection in vitro and in an animal model of neurodegeneration through a MEK-ERK and Akt-independent mechanism, *J Neurochem* **90** (2004), 595–608.
[65] A. Lorenzo and B.A. Yankner, Amyloid fibril toxicity in Alzheimer's disease and diabetes, *Ann N Y Acad Sci* **777** (1996), 89–95.
[66] T. Niikura, Y. Hashimoto, H. Tajima and I. Nishimoto, Death and survival of neuronal cells exposed to Alzheimer's insults, *J Neurosci Res* **70** (2002), 380–391.
[67] E. Tsukamoto, Y. Hashimoto, K. Kanekura, T. Niikura, S. Aiso and I. Nishimoto, Characterization of the toxic mechanism triggered by Alzheimer's amyloid-beta peptides via p75 neurotrophin receptor in neuronal hybrid cells, *J Neurosci Res* **73** (2003), 627–636.